International Journal of Mining and Geo-Engineering

IJMGE

IJMGE 53-2 (2019) 157-163

DOI: 10.22059/ijmge.2019.257534.594741

Estimation of xanthate decomposition percentage as a function of pH, temperature, and time by least squares regression and adaptive neuro-fuzzy inference system

Ali Behnamfard [a, *], Francesco Veglio [b]

[a] *Faculty of Engineering, University of Birjand, Birjand, South Khorasan, Iran*

[a] *Department of Industrial and Information Engineering and Economics, University of L'Aquila, Monteluco di Roio, L'Aquila, Italy*

Article History:

Received: 08 May 2018,

Revised: 13 December 2018

Accepted: 06 January 2019.

ABSTRACT

Estimating the xanthate decomposition percentage has a crucial role in the treatment of xanthate contaminated wastewaters and in the improvement of the flotation process performance. In this research, the modeling of xanthate decomposition percentage was performed using the least squares regression method and the Adaptive Neuro-Fuzzy Inference System (ANFIS). A multi-variable regression equation and the ANFIS models with various types and numbers of membership functions (MFs) were constructed, trained, and tested for the estimation of xanthate decomposition percentage. The statistical indices such as Root Mean Squared Error (RMSE), Mean Absolute Percentage Error (MAPE), and coefficient of determination (R^2) were used to evaluate the performance of various models. The lowest values of RMSE and MAPE and the closest value of R^2 to unity were determined for the ANFIS model with the triangular membership function and the number of input MFs 9 9 9 (0.766906, 3.553509 and 0.998793). This indicates that ANFIS is a powerful method in the estimation of xanthate decomposition percentage. The performance of new-adopted ANFIS data modeling was significantly better than the conventional least squares regression method.

Keywords : *Xanthate, Decomposition percentage, Estimation, ANFIS, Regression*

1. Introduction

The flotation process is widely used to up-grade base metal sulfide ores [1]. Annually, billion tons of sulfide ores are treated through this separation method and a huge amount of xanthate is used as the collecting agent in the flotation process [2]. Xanthates have a heteropolar molecular structure with a nonpolar hydrocarbon group and a polar head [2]. An electrochemical reaction occurs between the sulfide mineral surface and the polar head of xanthate [3]. This reaction makes the surface of sulfide minerals hydrophobic and it allows these mineral particles to be floated by air bubbles and be separated from other hydrophilic gangue minerals [4]. The dosage of xanthate in the flotation process varies in the range of 50 to 350 gr per ton of ore treated [5].

Decomposition percentage of xanthate can be determined through the following equation:

$$Decomposition\% = (1 - \frac{C_t}{C_0}) \times 100 \quad (1)$$

where C_0 (mg/L) is the initial concentration of xanthate in the solution and C_t (mg/L) is the xanthate concentration in the solution at time t.

The decomposition of xanthate in the flotation pulp can reduce its effective concentration [6]. The effective concentration of xanthate in the flotation pulp plays a crucial role in the floatability of sulfide minerals [6]. Furthermore, the decomposition products of xanthate can reduce the selectivity of a flotation process [6]. The stability of xanthate in aqueous solutions depends on several factors, especially the solution pH and temperature [6, 7]. In acidic aqueous solutions, xanthate undergoes hydrolysis to xanthic acid ($ROCS_2H$) which decomposes into carbon disulphide (CS_2) and alcohol (ROH) according to the following equations [8]:

$$ROCS_2^- + H_2O \rightarrow ROCS_2H + OH^- \quad (2)$$

$$ROCS_2H \rightarrow CS_2 + ROH \quad (3)$$

In neutral and alkaline media, the decomposition of xanthate occurs through hydrolytic decomposition according to the following reaction [8]:

$$6ROCS_2^- + 3H_2O \rightarrow 6ROH + CO_3^{2-} + 3CS_2 + 2CS_3^{2-} \quad (4)$$

As the solution temperature increases, the decomposition percentage of xanthate increases as well [9]. This is important due to the fact that the flotation of sulfide minerals is performed at various pulp temperatures during the summer and winter [6].

Although xanthates react selectively with the mineral surfaces in the ore pulp and are utilized at optimum dosages, excess and unreacted concentrations of these organosulfur compounds end up into the plant effluents [8]. Xanthates are toxic to aquatic life and therefore the release of xanthate contaminated wastewaters into the environment has sever environmental problems [10]. In recent years, several methods have been developed to remove xanthate from wastewaters, such as adsorption [10], chemical precipitation [11], chemical oxidation [8, 12-14], biodegradation [15, 16]. In natural degradation, chemical oxidation and biodegradation methods, the removal of xanthate is usually

* Corresponding author. Tel. +98-9151603400, *E-mail address:* behnamfard@birjand.ac.ir (A. Behnamfard).

performed through accelerating the degradation kinetics.

The estimation of xanthate decomposition percentage is highly crucial in sulfide mineral flotation and in the treatment of xanthate contaminated wastewaters, but it has not received enough attention up to now. In this research, we initially try to establish an equation for the estimation of xanthate decomposition percentage based on the process parameters including pH, temperature, and time by using the conventional least squares regression method. For this reason, the initially best subsets regression was applied using Minitab 17 software to identify a model with as few variables as possible and then the regression model was developed by multivariable regression. In this study, we also try to model the xanthate decomposition percentage by a new-adopted ANFIS data modeling procedure. ANFIS was first introduced by J. Jang in 1993 [17]. It is an artificial neural network that is based on the Takagi–Sugeno fuzzy inference system [17]. ANFIS has the potential to capture the benefits of both neural networks and the fuzzy logic in a single framework since it integrates the principles of both methods [18, 19]. ANFIS can be considered as a universal estimator since its inference system corresponds to a set of fuzzy IF–THEN rules that have a learning capability to approximate nonlinear functions [18, 19].

2. Methodology

2.1. Data

Table 1 shows the statistical parameters of the input and output data. The available dataset consisting of 1160 records was randomly divided into two subsets, the training set, and the testing set. Totally, 80% of the dataset (80%=929 data sets) was utilized for training the model and the remainder data points (20% =231 data sets) were utilized for the testing procedure. The datasets were extracted from previously published papers [6-9, 20-23].

Table 1. Description of input and output parameters in ANFIS and regression models.

Parameter	Description	Symbol	Range	Mean	Variance
Input	Solution temperature	Temp	283-300°K	294.85	3.76
	Solution pH	pH	2.18-9.98	7.75	3.92
	Time	Time	0.1-52350 min	13657.86	206818080
Output	Decomposition percentage	%decomposition	0-87.90%	37.51	492.53

2.2. Adaptive neuro-fuzzy inference system (ANFIS)

To describe an ANFIS system, it is simply surmized that the inference system has two inputs x and y and one output f. A first-order Sugeno fuzzy model has two rules as the following:

Rule 1. If x is A_1 and y is B_1, then $f_1 = p_1x + q_1y + r_1$. (5)

Rule 2. If x is A_2 and y is B_2, then $f_2 = p_2x + q_2y + r_2$. (6)

where p_1, p_2, q_1, q_2, r_1 and r_2 are linear parameters in the consequent part and A_1, A_2, B_1 and B_2 are nonlinear parameters [24].

Fig. 1 illustrates the corresponding equivalent ANFIS architecture for two input first-order Sugeno fuzzy model with two rules. The entire system architecture consists of five layers, including the fuzzy layer, product layer, normalized layer, de-fuzzy layer, and total output layer [25]. The node functions in the same layer are of the same function family as described in the following:

Layer 1: this layer is called the fuzzy layer. The adjustable nodes in this layer are represented by the square nodes and marked by A_1, A_2, B_1 and B_2 with x and y outputs. A_1, A_2, B_1 and B_2 are the linguistic labels (small, large, etc.) used in the fuzzy theory for dividing the MFs. The node functions in this layer that determine the membership relation between the input and output functions can be given by:

$$\begin{aligned} O_{1,i} &= \mu_{A_i}(x),\ i = 1,2 \\ O_{1,i} &= \mu_{B_{i-2}}(y),\ i = 3,4 \end{aligned} \quad (7)$$

where $O_{1,i}$ and $O_{1,j}$ denote the output functions, and $\mu_{Ai}(x)$ and $\mu_{Bi\text{-}2}(y)$ denote the appropriate MFs, which could be triangular, trapezoidal, Gaussian, generalized bell functions [24]. The MFs are defined as follows:

A triangular MF is specified by three parameters {a, b, c} as follows [25]:

$$\mu_{A_i}(x) = \begin{cases} 0, & x \le a. \\ \dfrac{x-a}{b-a}, & a \le x \le b. \\ \dfrac{c-x}{c-b}, & b \le x \le c \\ 0, & c \le x. \end{cases} \quad (8)$$

The parameters {a, b, c} (with a < b < c) determine the x coordinates of the three corners of the underlying triangular MF.

A trapezoidal MF is specified by four parameters {a, b, c, d} as follow [25]:

$$\mu_{A_i}(x) = \begin{cases} 0, & x \le a. \\ \dfrac{x-a}{b-a}, & a \le x \le b. \\ 1, & b \le x \le c \\ \dfrac{d-x}{d-c}, & c \le x \le d. \\ 0, & d \le x. \end{cases} \quad (9)$$

The parameters {a, b, c, d} (with a < b <= c < d) determine the x coordinates of the four corners of the underlying trapezoidal MF. A Gaussian MF is specified by two parameters as follows [25]:

$$\mu_{A_i}(x) = \exp\left(-\frac{(x-c)^2}{2\sigma^2}\right) \quad (10)$$

A Gaussian MF is determined complete by c and σ; c represents the MFs center and σ determines the MFs width.

A generalized bell MF is specified by three parameters {a, b, c} as follows [24]:

$$\mu_{A_i}(x) = \frac{1}{1+\left(\dfrac{x-c}{a}\right)^{2b}} \quad (11)$$

where parameter b is usually positive.

Layer 2: this is the product layer and each node is a fixed node marked by a circle node and labeled by Prod. The outputs w_1 and w_2 are the weight functions of the next layer. The output of this layer, $O_{2,i}$, is the product of all incoming signals and is given by:

$$O_{2,i} = w_i = \mu_{A_i}(x)\mu_{B_i}(y),\ i = 1,2 \quad (12)$$

The output signal of each node, w_i, represents the firing strength of a rule [24].

Layer 3: this is the normalized layer and each node in this layer is a fixed node, marked by a circle node and labeled by Norm. The nodes normalize the firing strength by estimating the ratio of firing strength for this node to the sum of all firing strengths, i.e.

$$O_{3,i} = \overline{w_i} = \frac{w_i}{w_1 + w_2},\ i = 1,2. \quad (13)$$

Layer 4: This is the de-fuzzy layer having adaptive nodes and marked by square nodes. Each node i in this layer is an adaptive node with a node function:

$$O_{4,i} = \overline{w_i} f_i = w_i(p_i x + q_i y + r_i),\ i = 1,2 \quad (14)$$

where $\overline{w_i}$ is the normalized firing strength output from layer 3 and p_i, q_i and r_i are the parameters set of this node. These parameters are linear and referred as consequent parameters of this node [24].

Layer 5: The single node in this layer is a fixed node marked by circle node and labeled sum, which computes the overall output as the summation of all incoming signals:

$$O_{5,i} = \sum_i \overline{w}_i f_i = \frac{\sum_i w_i f}{w_1 + w_2}, \quad i = 1,2 \tag{15}$$

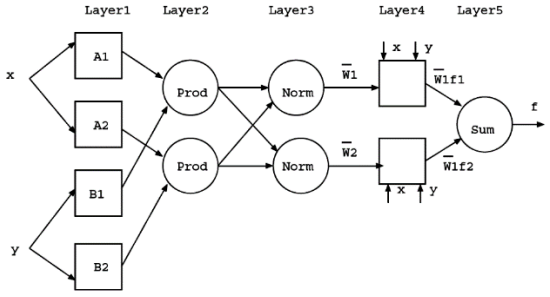

Fig 1. An ANFIS network structure for a simple FIS.

An ANFIS network can be trained based on supervised learning to reach from a specific input to a definite target output. In the forward pass of the hybrid algorithm of ANFIS, the node outputs go forward until the fourth layer and consequent linear parameters, (p_i, q_i, r_i), are found by the least-squares method using the training dataset. The error signals propagate backwards in the pass and the premise nonlinear parameters, (a_i, b_i, c_i) are updated by the gradient descent. It has been proven that this hybrid algorithm is highly efficient in training ANFIS models [26].

2.3. Development of ANFIS models

To model the decomposition percentage of xanthate, a network with three inputs was selected, with input variables corresponding to the solution temperature, pH, and time (Fig. 2).

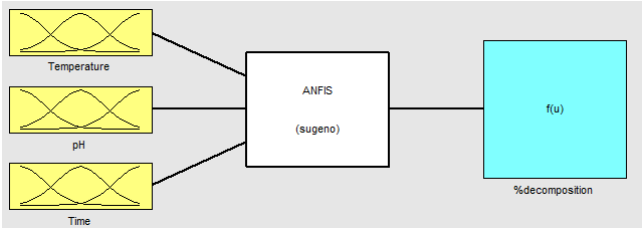

Fig 2. System ANFIS: 3 inputs (Temperature, pH, and Time), 1 output (decomposition percentage)

The applicability of ANFIS models to estimate the decomposition percentage of xanthate was validated by the following criteria:

Root Mean Squared Error (RMSE) [27]:

$$RMSE = \sqrt{\frac{1}{N}\sum_{t=1}^{N}(A_t - F_t)^2} \tag{16}$$

where A_t and F_t are actual and predicted values, respectively, and N is the number of training or testing samples.

Mean Absolute Percentage Error (MAPE) [27]:

$$MAPE = \frac{1}{N}\sum_{t=1}^{N}\left|\frac{A_t - F_t}{A_t}\right| \times 100 \tag{17}$$

Coefficient of determination (R^2) [27]:

$$R^2 = 1 - \frac{\sum_{t=1}^{N}(A_t - F_t)^2}{\sum_{t=1}^{n}(A_t - \overline{A})^2} \tag{18}$$

Where, $\overline{A} = \frac{1}{N}\sum_{t=1}^{N} A_t$ is the average value of A_t over the training or testing datasets. The lower RMSE and MAPE values and closer R^2 value to unity mean better performance of the models.

The best subsets regression approach is an efficient way to identify the models that achieve our goals with as few predictors as possible. This method identifies the subset models that produce the highest R^2 values from a full set of the predictor variables that we specify. Subset models may actually estimate the regression coefficients and predict future responses with smaller variance than the full model using all predictors [28]. Minitab examines all possible subsets of the predictors, beginning with all models containing one predictor, and then all models containing two predictors, and so on [28]. Table 2 shows the results of best subsets regression performed by Minitab 17. Each row in the table represents information about one of possible regression models. The first column—labeled Vars—shows how many predictors are in the model. The last three columns show which predictors are in the model. If an "X" appears in the row, it will include in the model as the predictor. The other five columns—labeled R^2, R^2 (adj), R^2 (pred), Cp, and S— pertain to the criteria that we use in deciding which models are "best."

3. Results and Discussion

3.1. Estimation of xanthate decomposition percentage by Least Square Regression Method

The effect of solution pH and temperature on the decomposition rate of xanthate is shown in Fig. 3. As seen, the decomposition rate of xanthate increases by increasing the solution temperature. The decomposition rate of xanthate drastically increases by decreasing the solution pH from 7.95 to 4.15 and to a lesser extent by increasing the solution pH from 7.95 to 9.95.

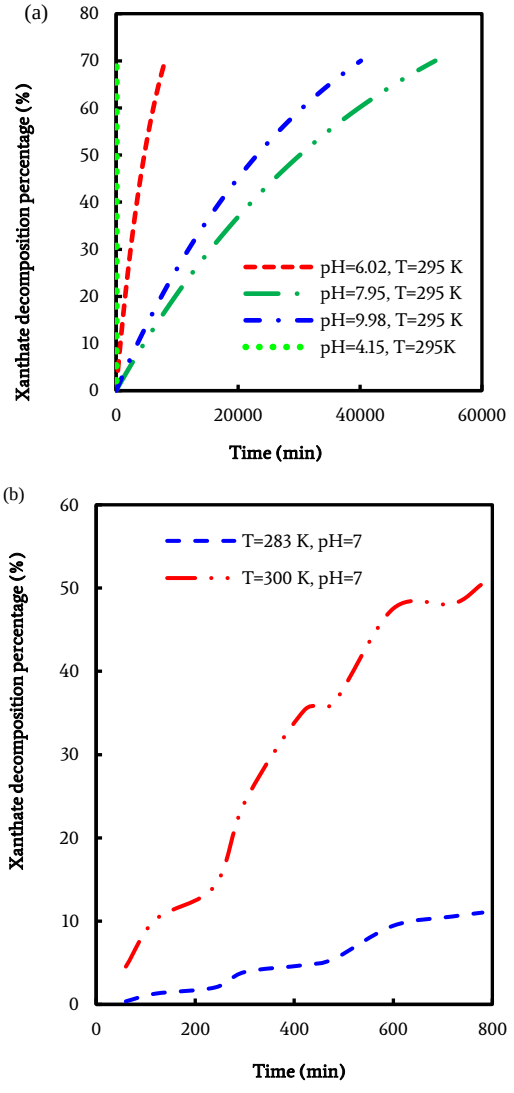

Fig 3. The effect of a) solution pH and b) solution temperature on the decomposition rate of xanthate

The model with all the variables has the highest R^2 (58%) and adjusted R^2 (57.9%), and the lowest Mallows' Cp value (4.0) and S value

(14.402). Hence, the model with all the variables can be considered as the best model for the estimation of xanthate decomposition percentage at different solution conditions.

Table 2 The results of best subsets regression

Vars	R^2	R^2 (adj)	R^2 (pred)	Mallows Cp	S	Temp	pH	Time
1	40.8	40.8	40.7	473.9	17.084			X
2	1.8	1.7	1.5	1550.8	22.013	X		
3	0.6	0.5	0.2	1583.9	22.148		X	
4	57.3	57.2	57.1	22.6	14.523		X	X
5	41.6	41.5	41.3	455.4	16.984	X		X
6	2.4	2.3	2.0	1534.8	21.950	X	X	
7	58.0	57.9	57.8	4.0	14.402	X	X	X

The general regression was applied by Minitab 17 to fit least squares models to understand the relationship between the decomposition percentage of xanthate and the predictors' variables including temperature, pH, and time. Eq. 19 shows the relevant equation.

$$\text{Decomposition \%} = 0.24298\ \text{Temp} - 26.1\ \text{pH} - 0.205\ \text{Time} + 0.0654\ \text{Temp*pH} + 0.000692\ \text{Temp*Time} + 0.000283\ \text{pH*Time} \quad (19)$$

Table 3 shows the analysis of variance (ANOVA) table and the model summery for the multi-variable regression model. As can be seen, the p-value for the regression model is 0.000 in the ANOVA table which indicates that the equation is statistically significant at an α-level of .05. Furthermore, the value of R^2, R^2 (adj), and R^2 (pred) is 0.9041, 0.9036, and 0.9031, respectively. These values are close to unity which further confirm that the model is significant at 95% confidence level for the estimation of xanthate decomposition percentage.

Table 3 ANOVA table and the model summary for the multi-variable regression model.

Analysis of Variance

Source	DF	Adj SS	Adj MS	F-Value	P-Value
Regression	6	1993645	332274	1815.09	0.000
Temp	1	255187	255187	1393.99	0.000
pH	1	463	463	2.53	0.112
Time	1	135	135	0.74	0.391
Temp*pH	1	253	253	1.38	0.240
Temp*Time	1	133	133	0.73	0.394
pH*Time	1	28288	28288	154.53	0.000
Error	1155	211437	183		
Total	1161	2205081			

Model Summary

S	R-sq	R-sq(adj)	R-sq(pred)
13.5300	90.41%	90.36%	90.31%

Coefficients

Term	Coef	SE Coef	T-Value	P-Value	VIF
Temp	0.24298	0.00651	37.34	0.000	23.35
pH	-26.1	16.4	-1.59	0.112	109208.27
Time	-0.205	0.239	-0.86	0.391	1.42938E+08
Temp*pH	0.0654	0.0557	1.17	0.240	109252.52
Temp*Time	0.000692	0.000811	0.85	0.394	1.42936E+08
pH*Time	0.000283	0.000023	12.43	0.000	100.06

In order to further validate the relevant equation, the histogram and the normal probably plot of residuals, the plot of residual versus fitted values and the plot of residual versus the run order were plotted (Fig. 4). The histogram of residuals has a bell shape which confirms the normal distribution of the residuals. The normal probability plot shows an approximately linear pattern which is consistent with normal distributions. The plot of residual versus fitted values shows a random pattern, which confirms the constant variance of the residuals. The residual versus order plot displays the order that the data was collected and can be used to find the non-random error, especially of time-related effects. The residual versus order plot shows a random pattern which indicates the time-independent variance of residuals.

3.2. The estimation of xanthate decomposition percentage by ANFIS

In this research, a hybrid grid partitioning ANFIS was applied for the estimation of xanthate decomposition percentage as a function of solution temperature, pH, and time. To evaluate the effect of MF type on the performance of ANFIS models, it was set as Triangular, Trapezoidal, Generalized bell, and Gaussian. The number of input MFs was set 3 3 3. Fig. 5 shows the general structure of ANFIS models. The characteristics of ANFIS models are shown in Table 4.

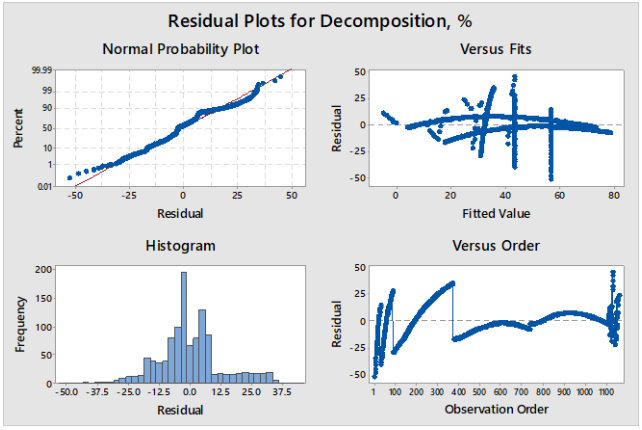

Fig.4 Residual plots for decomposition percentage of xanthate

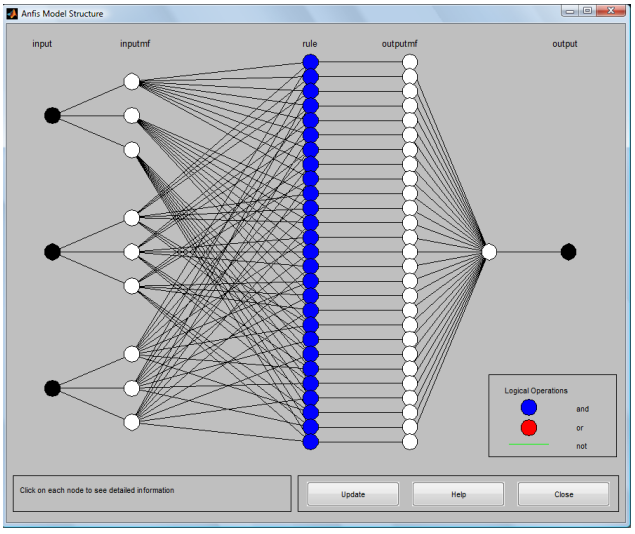

Fig.5 ANFIS model structure used for estimation of xanthate decomposition percentage

Table 4 Parameter types of ANFIS models with different MF types.

ANFIS parameter type	Membership Function Type			
	Triangular	Trapezoidal	Generalized bell	Gaussian
Number of MFs	3 3 3	3 3 3	3 3 3	3 3 3
Output MF	Linear	Linear	Linear	Linear
Number of nods	78	78	78	78
Number of linear parameters	108	108	108	108
Number of nonlinear parameters	27	36	27	18
Total number of parameters	135	144	135	126
Number of training data pairs	929	929	929	929
Number of testing data pairs	231	231	231	231
Number of fuzzy rules	27	27	27	27
Number of epochs	100	100	100	100
Training error	0.9978	4.4248	1.378	1.34923

The proposed ANFIS models were trained separately for 100 epochs by using various MFs and their performance was compared in terms of RMSE, MAPE, and coefficient of determination (R^2) for the training and testing data sets. The results are presented in Table 5. The lowest RMSE and MAPE values and the closet value of coefficient of determination (R^2) to unity are observed for the triangular MF for both of training and testing data set. Hence, the ANFIS model with triangular MF is a more accurate and consistent method for the estimation of decomposition

percentage of xanthate than the other ANFIS models.

Table 5 Performances of ANFIS models with different MFs in estimation of xanthate decomposition percentage

Membership function	Training data set			Testing data set		
	RMSE	MAPE (%)	R^2	RMSE	MAPE (%)	R^2
Triangular	0.997799	5.114386	0.997986	1.052606	6.403248	0.997726
Trapezoidal	4.424813	119.5478	0.960386	4.279191	101.7817	0.962419
Gaussian	1.34923	7.374592	0.996317	1.284703	7.389331	0.996613
Generalized bell	1.378041	9.23183	0.996158	1.31637	8.902129	0.996444

Fig. 6 shows the applicability of ANFIS models by different MF types for the estimation of xanthate decomposition percentage. The ANFIS model with triangular MF is clearly the most accurate and powerful method for the estimation of xanthate decomposition percentage.

In order to evaluate the effect of number of input MFs on the performance of ANFIS models, various models are constructed with different number of input MFs. Based on the previous results the MF type was triangular. Table 6 shows the characteristics of different ANFIS models.

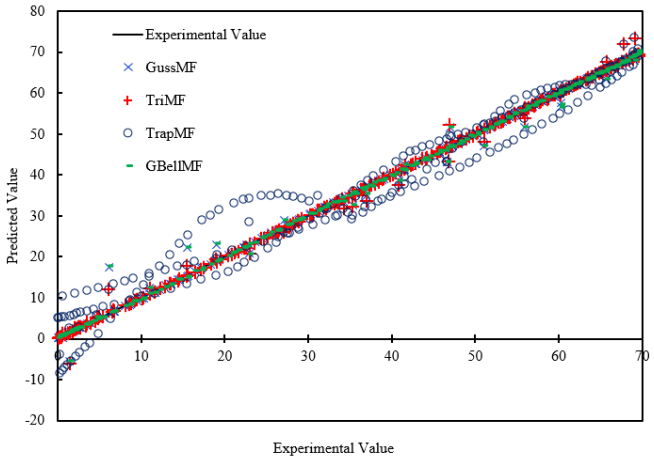

Fig.6 Predicted xanthate decomposition percentage by different ANFIS models vs. experimental values.

Table 6 Parameter types of ANFIS models with different number of input MFs.

No. of input MFs	ANFIS parameter type									
	Output MF	No. of nods	No. of linear parameters	No. of nonlinear parameters	Total number of parameters	No. of training data pairs	No. of testing data pairs	No. of fuzzy rules	No. of epoch	Training error
3 3 3	Linear	78	108	27	135	929	231	27	100	0.9978
6 3 3	Linear	138	216	36	252	929	231	54	100	1.00017
3 6 3	Linear	138	216	36	252	929	231	54	100	0.94426
3 3 6	Linear	138	216	36	252	929	231	54	100	0.99893
6 6 3	Linear	252	432	45	477	929	231	108	100	0.94363
6 3 6	Linear	252	432	45	477	929	231	108	100	0.99542
3 6 6	Linear	252	432	45	477	929	231	108	100	0.80468
6 6 6	Linear	474	864	54	918	929	231	216	100	0.80186
9 6 6	Linear	696	1296	63	1359	929	231	324	100	0.79515
6 9 6	Linear	696	1296	63	1359	929	231	324	100	0.76384
6 6 9	Linear	696	1296	63	1359	929	231	324	100	0.70979
9 9 6	Linear	1026	1944	72	2016	929	231	486	100	0.75768
9 6 9	Linear	1026	1944	72	2016	929	231	486	100	0.70355
6 9 9	Linear	1026	1944	72	2016	929	231	486	100	0.68977
9 9 9	Linear	1518	2916	81	2997	929	231	729	100	0.68522

The performance of various ANFIS models with different number of input MFs was compared based on RMSE, MAPE, and R^2 criteria for the training and testing datasets and the results are presented in Table 7. The model performance improves by increasing the number of input MFs so that the lower values of RMSE and MAPE and closer R^2 value to unity are obtained at higher numbers of input MFs.

Fig. 7 shows the final rules of the fuzzy inference system by using the triangular MF. The trained IF–THEN rules can be used for the estimation of xanthate decomposition percentage at different solution temperatures and pH values and at different time intervals. In other words, if we change the values of inputs (i.e., Temperature, pH, and Time) in the input box (down left side of Fig.7), then we can immediately find the corresponding decomposition percentage of xanthate.

3.3. Comparison between ANFIS and the statistical method

A comparison between ANFIS and the statistical model was made and the results are presented in Table 8 and Fig. 8. The comparison between ANFIS and least square regression methods through RMSE, MAPE, and R^2 criteria shows that ANFIS is a more powerful method for the estimation of xanthate decomposition percentage than the least square regression method. Furthermore, Fig. 8 clearly shows that the the estimation of xanthate decomposition percentage by ANFIS is significantly more accurate than that of the regression method.

Table 7 Performance of ANFIS models with different number of input MFs in estimation of xanthate decomposition percentage

No. of input MFs	Training data set			Testing data set		
	RMSE	MAPE (%)	R^2	RMSE	MAPE (%)	R^2
3 3 3	0.997799	5.114386	0.997986	1.052606	6.403248	0.997726
6 3 3	1.000172	5.194478	0.997976	1.054964	6.469476	0.997716
3 6 3	0.944257	4.426145	0.998196	0.995175	5.837537	0.997967
3 3 6	0.998929	3.156303	0.997981	1.053362	4.83931	0.997723
6 6 3	0.943629	4.332312	0.998198	0.994815	5.764674	0.997969
6 3 6	0.995422	2.986689	0.997995	1.050147	4.687518	0.997737
3 6 6	0.804678	2.478982	0.99869	0.868791	4.286556	0.998451
6 6 6	0.80186	2.429795	0.998699	0.866439	4.248398	0.998459
9 6 6	0.79515	2.414279	0.998721	0.860694	4.238341	0.99848
6 9 6	0.763836	2.323379	0.99882	0.831903	4.170483	0.99858
6 6 9	0.709791	1.753631	0.998981	0.787767	3.627235	0.998726
9 9 6	0.757666	2.301569	0.998839	0.826724	4.153399	0.998597
9 6 9	0.703557	1.735269	0.998998	0.783033	3.615325	0.998742
6 9 9	0.68977	1.664708	0.999037	0.770085	3.562222	0.998783
9 9 9	0.685223	1.650587	0.99905	0.766906	3.553509	0.998793

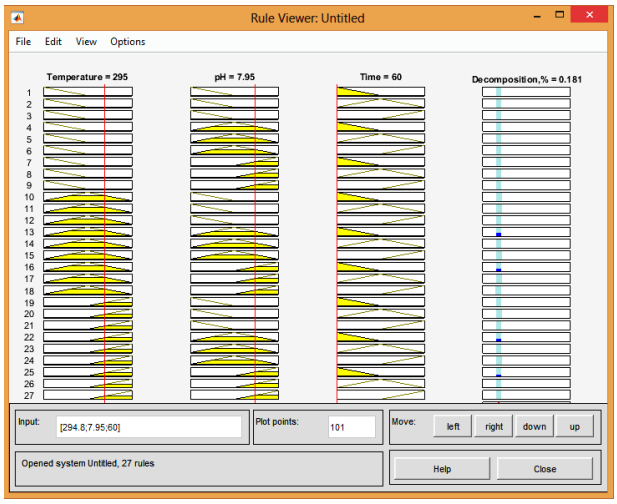

Fig.7 IF–THEN rules after training that can be used for the estimation of xanthate decomposition percentages at different solution conditions.

Table 8 The comparison between ANFIS model (Triangular MF and number of input MFs 9 9 9) with least squares regression model in the estimation of xanthate decomposition percentage

Modeling Method	Training data set			Testing data set		
	RMSE	MAPE (%)	R^2	RMSE	MAPE (%)	R^2
Regression	14.3683	210.5587	0.582291	13.63942	192.4572	0.618196
ANFIS	0.685223	1.650587	0.99905	0.766906	3.553509	0.998793

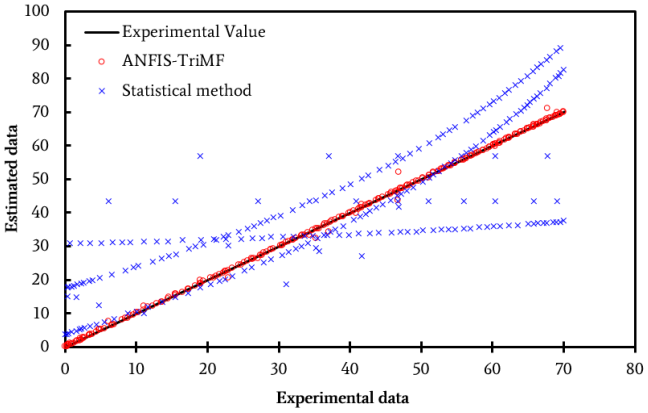

Fig.8 The estimated xanthate decomposition percentage by ANFIS-TriMF and statistical methods vs. experimental data.

4. Conclusion

In this research, the estimation of xanthate decomposition percentage was carried out based on the solution temperature, pH, and time through the least squares regression and ANFIS methods. The best subsets regression in the Minitab 17 package indicated that the model with all of the variables has the highest R^2 (58%) and adjusted R^2 (57.9%), and the lowest Mallows' Cp value (4.0) and S value (14.402). The least squares regression through general regression by Minitab 17 proposed the following equation for the estimation of xanthate decomposition percentage:

Decomposition % = 0.24298 Temp – 26.1 pH – 0.205 Time + 0.0654 Temp×pH + 0.000692 Temp×Time + 0.000283 pH×Time

The validity of the model was confirmed through an analysis of the variance table and residual plots.

Different ANFIS models were constructed with various types and numbers of MF and the best results were obtained by Triangular MF and the number of input MFs 9 9 9. The low values of RMSE and MAPE (0.77 and 3.55%) for this model confirmed the ability of this model in the estimation of xanthate decomposition percentage. The rule viewer GUI after training can be easily applied for the estimation of xanthate decomposition percentage at any point of temperature, pH, and time.

The comparison of ANFIS and the statistical method revealed that the ANFIS model is a more powerful method than the statistical method for the estimation of xanthate decomposition percentage.

REFERENCES

[1] Fuerstenau, M.C., Chander, S., Woods, R., 2007. Sulfide mineral flotation. In: Fuerstenau, M.C., Jameson, G., Yoon, R. H., (Eds.), Froth flotation a century of innovation. Society for Mining, Metallurgy, and Exploration, Inc. (SME), Littleton, Colorado, pp. 425-464.

[2] Bulatovic, S.M., 2007. Handbook of Flotation Reagents. 1st ed. Elsevier, Amsterdam.

[3] Wang, D., 2016. Flotation reagents: Applied surface chemistry on minerals flotation and energy resources beneficiation, Springer, Singapore, pp. 9-38.

[4] Wills, B. A. and Napier-Munn, T., 2006. Wills' mineral processing technology: An introduction to the practical aspects of ore treatment and mineral recovery, 7th, Elsevier, Amsterdam, pp. 267-352.

[5] NICNAS, 2000. Sodium Ethyl Xanthate: Priority Existing Chemical Secondary Notification Assessment, Australian Government Pub. Service, Australia, Canberra, Australia.

[6] Sun Z., Forsling, W., (1997). The degradation kinetics of ethyl-xanthate as a function of pH in aqueous solution. *Minerals Engineering*, 10 (4), 389-400.

[7] Trudgett, M., 2005. The ultra-trace level analysis of xanthates by high performance liquid chromatography, M.Sc. Thesis, University of Western Sydney, Australia.

[8] Molina, G. C., Cayo, C. H., Rodrigues, M. A. S., Bernardes, A. M., (2013). Sodium isopropyl xanthate degradation by advanced oxidation processes, *Minerals Engineering*, 45, 88–93.

[9] Shen, Y., Nagaraj, D.R., Farinato, R., Somasundaran, P., (2016). Study of xanthate decomposition in aqueous solutions, *Minerals Engineering*, 93, 10-15.

[10] Oliveira, C.R., Rubio, J., (2009). Isopropylxanthate ions uptake by modified natural zeolite and removal by dissolved air flotation, *International Journal of Mineral Processing*, 90, 21–26.

[11] Mielczarski, J., (1986). The role of impurities of sphalerite in the adsorption of ethyl xanthate and its flotation. *International Journal of Mineral Processing*, 16(3/4), 179–194.

[12] Silvester, E., Truccolo, D., Fu, P., (2002). Kinetics and mechanism of the oxidation of ethyl xanthate and ethyl thiocarbonate by hydrogen peroxide. *Journal of the Chemical Society, Perkin Transactions*, 2, 2(9), 1562–1571.

[13] Fagadar-Cosma, G., Taranu, I., Fagadar-Cosma, E., (2003). Electrochemical oxidation of sodium ethyl xanthate in aqueous solutions. *Revue Roumaine de Chimie*, 48(2), 131–136.

[14] Jin, X., Shui-yu, S., Ping, Z., He-shan, C., (2005). Degradation of remainder xanthate in flotation wastewater by fenton reagent. *Environmental Protection of Chemical Industry*, 25(2), 125–127.

[15] Deo, N., Natarajan, K. A., (1998). Biodegradation of some organic flotation reagents by bacillus polymyxa. *Bioremediation Journal*, 2(3), 205-214.

[16] Chockalingam, E., Subramanian, S., Natarajan, K.A., (2003). Studies on biodegradation of organic flotation collectors using Bacillus polymyxa, *Hydrometallurgy*, 71, 249–256.

[17] Jang, J. (1993). ANFIS: Adaptive network-based fuzzy inference systems. *IEEE Transactions on Systems, Man, and Cybernetics*, 23, 665-683.

[18] Mathur, N., Glesk, I., Buis, A., (2016). Comparison of adaptive neuro-fuzzy inference system (ANFIS) and Gaussian processes for machine learning (GPML) algorithms for the prediction of skin temperature in lower limb prostheses. *Medical Engineering & Physics*, 38(10), 1083–1089.

[19] Atia, D. M., El-madany, H. T., (2017). Analysis and design of greenhouse temperature control using adaptive neuro-fuzzy inference system, *Journal of Electrical Systems and Information Technology*, 4(1), 34-48.

[20] Mustafa, S., Hamid, A., Naeem, A., Sultana, Q., (2004). Effect of pH, temperature and time on the stability of potassium ethyl xanthate. *Journal of the Chemical Society of Pakistan*, 26(4), 363-366.

[21] Chen, X., Hu, Y., Peng, H., Cao, X., (2015). Degradation of ethyl xanthate in flotation residues by hydrogen peroxide. *Journal of Central South University*, 22, 495-501.

[22] Shen, Y., Nagaraj, D.R., Farinato, R., Somasundaran, P., (2016). Study of xanthate decomposition in aqueous solutions. *Minerals Engineering*, 93, 10–15.

[23] Iwasaki, I., Cooke, S.R.B., (1958). The Decomposition of Xanthate in Acid Solution. *Journal of the American Chemical Society*, 80(2), 285-288.

[24] Esen, H., Inalli, M., Sengur, A., Esen, M., (2008). Modelling a ground-coupled heat pump system using adaptive neuro-fuzzy inference systems. *International Journal of Refrigeration*, 31, 65–74.

[25] Guney, K., Sarikaya, N., (2009). Comparison of adaptive-network-based fuzzy inference systems for bandwidth calculation of rectangular microstrip antennas. *Expert Systems with Applications*, 36, 3522–3535.

[26] Zounemat-Kermani, M., Teshnehlab, M., (2008). Using adaptive neuro-fuzzy inference system for hydrological time series prediction. *Applied Soft Computing*, 8, 928–936.

[27] Wang, Y.M., Elhag, T. M. S., (2008). An adaptive neuro-fuzzy inference system for bridge risk assessment. *Expert Systems with Applications*, 34, 3099–3106.

[28] Basics of best subsets regression (2016). Retrieved 7 March 2017, from http://support.minitab.com/en-us/minitab/17/topic-library/modeling-statistics/regression-and-correlation/basics/basics-of-best-subsets-regression/